Improved Brønsted Acidity of Mesoporous [Al]MCM-41 Material Treated with Ammonium Fluoride[†]

Mingcan Xu, Wei Wang, Michael Seiler, Andreas Buchholz, and Michael Hunger*

Institute of Chemical Technology, University of Stuttgart, D-70550 Stuttgart, Germany

Received: November 15, 2001; In Final Form: January 23, 2002

Mesoporous [Al]MCM-41 material ($n_{Si}/n_{Al} = 15$) has been modified by an aqueous solution of ammonium fluoride and characterized by XRD, N_2 adsorption, ^1H, ^{19}F, ^{27}Al, and ^{29}Si NMR spectroscopies and tested in the conversion of 2-propanol. By $^1H\{^{27}Al\}$ TRAPDOR MAS NMR it is shown that a significant number of SiOH groups (1.8 ppm) in the dehydrated parent [Al]MCM-41 material is located in the vicinity of aluminum atoms. After a weak treatment of the [Al]MCM-41 material with NH_4F, a ^{19}F NMR signal of Si−F species at −156 ppm and a transformation of tetrahedrally coordinated framework aluminum (^{27}Al NMR signal at 53 ppm) to octahedrally coordinated aluminum (^{27}Al NMR signal at 0 ppm) were observed in the spectra of hydrated samples. In addition, an enhanced catalytic activity was found accompanied by a low-field shift and an intensity decrease of the ^1H NMR signal of SiOH groups in dehydrated samples. A model is proposed that explains the enhanced catalytic activity and the improved number of hydroxyl groups acting as Brønsted acid sites in weakly modified and dehydrated [Al]MCM-41 materials by the formation of $Si(O_2F)OH$ species in the vicinity of strongly disturbed framework aluminum atoms. Simultaneously, an incorporation of fluorine atoms in the local structure of framework aluminum occurs. A strong treatment with NH_4F leads to a damage of the mesoporous structure.

Introduction

Mesoporous MCM-41 materials are amorphous silicates and metal-silicates with uniform pores and long-range order, which attract wide attention in heterogeneous catalysis and adsorption technologies.[1] The pore sizes of MCM-41 materials of up to 10 nm are ideal for the processing of molecules having diameters larger than those of micropores in zeolites. Hitherto, numerous methods have been applied to introduce desired catalytic and adsorptive properties of these materials.[2] Unlike zeolites, aluminum containing mesoporous MCM-41 materials ([Al]-MCM-41) have a weak Brønsted acidity only.[3−5] The activity of [Al]MCM-41 for reactions catalyzed by Brønsted acid sites, e.g., *n*-heptane cracking, is much lower than that of zeolites H−Y and USY, but similar to that of amorphous silica−alumina.[5] On the other hand, [Al]MCM-41 is reported as a suitable catalyst for the conversions of 1,3,5-triisopropylbenzene and cumene, which proceed predominantly via catalytic cracking.[6] The incorporation of other trivalent elements, such as B, Ga, and Fe, leads to materials with lower catalytic activity than that of [Al]MCM-41.[7]

To obtain acidic mesoporous [Al]MCM-41 catalysts suitable for the processing of large hydrocarbons, a modification of their hydroxyl groups is desirable. As shown in previous studies of modified zeolites, fluoridation improves both the number of hydroxyl groups acting as Brønsted acid sites and the catalytic activity of these materials.[8,9] In the present work, therefore, mesoporous [Al]MCM-41 material was modified with ammonium fluoride and characterized by XRD, N_2 adsorption, multinuclear solid-state NMR spectroscopy and the conversion of 2-propanol.

Experimental Section

The synthesis of the mesoporous [Al]MCM-41 material was performed as described elsewhere:[10] 0.71 g sodium aluminate (Riedel-de Häen) dissolved in 5.0 g deionized water, 37.4 g water glass (Merck, 25.5−28.5% SiO_2, 7.5−8.5% Na_2O), 32.0 g tetradecyltrimethylammonium bromide (Sigma), and 2.3 g sulfuric acid (98%, Merck) diluted in 10.1 g water were added to 115.2 g deionized water. The gel obtained was placed into an autoclave and kept at 423 K for about 11 h. The product was filtered and washed with ethanol and deionized water. This material was calcined, first under flowing nitrogen (480 mL/min) at 773 K, and then under air until the product appeared white. The calcined product was 3-fold exchanged in an aqueous solution of 0.1 M ammonium nitrate (5 g:100 g) at 353 K for 3 h to obtain the ammonium-exchanged form of [Al]MCM-41. Subsequently, the ammonium-exchanged product was dried under air at 393 K overnight. This parent [Al]MCM-41/0 material has a silicon-to-aluminum ratio of $n_{Si}/n_{Al} = 15$ (AES-ICP). Portions of 1 g of the parent [Al]MCM-41/0 material were stirred in different amounts of an aqueous solution of 0.1 M ammonium fluoride at room temperature for 30 h, then dried at 353 K overnight and calcined under air at 723 K for 8 h. The samples obtained were labeled as [Al]MCM-41/*n*, where *n* is the number of fluorine atoms introduced by the treatment (see Table 1, first and second column). This number of fluorine atoms is given in mmol/g and was calculated according to the amount of NH_4F added to the [Al]MCM-41 materials.

X-ray powder diffraction patterns were recorded using a Siemens D5000 instrument using CuKα-radiation and a scan step width of 0.02°. Before the N_2 adsorption/desorption isotherms were measured at 77 K on a Micromeritics ASAP 2010 instrument, all samples were degassed ($p < 10^{-2}$ Pa) at 523 K for 3 h.

Acidity of Mesoporous [Al]MCM-41 Material

J. Phys. Chem. B, Vol. 106, No. 12, 2002 **3203**

TABLE 1: Assignment of the Parent and Modified Mesoporous [Al]MCM-41 Materials and Their Characterization by N_2 and NH_3 Adsorption and ^1H MAS NMR Spectroscopy: The Parent [Al]MCM-41/0 Has a Total OH Concentration of 1.9 mmol/g

samples	introduced NH_4F in mmol/g	BET area in m^2/g	ammonium ions at 6.7 ppm in mmol/g[a]
[Al]MCM-41/0	0	1069	0.18
[Al]MCM-41/0.07	0.07	1108	0.23
[Al]MCM-41/0.12	0.12	1130	0.19
[Al]MCM-41/0.28	0.28	1135	0.28
[Al]MCM-41/0.44	0.44	1148	0.40
[Al]MCM-41/0.66	0.66	1056	0.27
[Al]MCM-41/1.05	1.05	974	0.27
[Al]MCM-41/1.64	1.64	892	0.18
[Al]MCM-41/2.17	2.17	797	0.19

[a] Experimental accuracy ±10%.

Magic angle spinning (MAS) NMR investigations were performed on Bruker spectrometers MSL 300 and MSL 400 at resonance frequencies of 400.1 MHz for ^1H ($\nu_{rot} = 8$ kHz), 282.2 MHz for ^{19}F ($\nu_{rot} = 3.5$ kHz) and 79.5 MHz for ^{29}Si nuclei ($\nu_{rot} = 3.5$ kHz). The ^{27}Al MAS NMR ($\nu_{rot} = 10$ kHz) and spin−echo spectra were recorded at 104.2 MHz. A p_1-τ-p_2-τ-echo-sequence was applied with p_1 and p_2 pulses of 0.61 μs and a pulse delay of $\tau = 10$ μs. The ^1H{^{27}Al}-TRAPDOR MAS NMR experiments were performed as described elsewhere[11,12] by irradiating a ^{27}Al pulse with an rf field of 50 kHz in the first pulse delay τ of the $\pi/2$-τ-π-τ pulse sequence (Hahn echo) applied to the ^1H nuclei ($\nu_{rot} = 5$ kHz; $\tau = 200$ ms). Before the ^1H MAS NMR investigations and the adsorption of NH_3, all samples were dehydrated at 673 K for 12 h at a pressure of lower than 10^{-2} mbar. The adsorption of NH_3 was performed at room temperature with a partial pressure of 200 mbar for 6 h until the pressure of NH_3 remained constant. After adsorption, the samples were heated at 473 K for 2 h to remove physically adsorbed ammonia. Quantitative ^1H MAS NMR measurements were performed using an external intensity standard (35% ion-exchanged zeolite H,Na−Y). ^1H and ^{29}Si NMR signals were referred to TMS (tetramethylsilane), ^{19}F NMR signals to $CFCl_3$ and ^{27}Al NMR signals to an 0.5 M aqueous solution of aluminum nitrate. Before the ^{19}F and ^{27}Al NMR measurements, the samples were hydrated overnight in a desiccator.

The conversion of 2-propanol was performed in a fixed-bed reactor with an inner diameter of 5 mm, under atmospheric pressure, with a modified residence time of $W/F = 32$ g h/mol and at a reaction temperature of 433 K. Before starting the catalytic reaction, the samples were activated in flowing nitrogen (100 mL/min) at 673 K for 12 h. The reaction products were analyzed by on-line gas chromatography using a gas chromatograph HP 6890 (Hewlett-Packard) and a 30 m DB-WAX column (J&W Scientific).

Results and Discussion

Investigations of the Long-range Order and Pore Structure. The XRD pattern of the parent [Al]MCM-41/0 material, in Figure 1, shows three peaks attributed to the (100), (110), and (200) reflections of the long-range ordered hexagonal structure. After a stronger treatment with NH_4F, a decrease of the corresponding peaks in the XRD patterns occurred indicating a damage of the mesoporous structure. This finding is in line with the pore size distributions (Figure 2) and the BET areas (Tab. 1, column 3) determined by adsorption of N_2. While the mean pore size of the parent [Al]MCM-41/0 material amounts to ca. 2.5 nm, this value decreases to about 2.0 nm after treatment with 2.17 mmol NH_4F per gram ([Al]MCM-41/2.17)
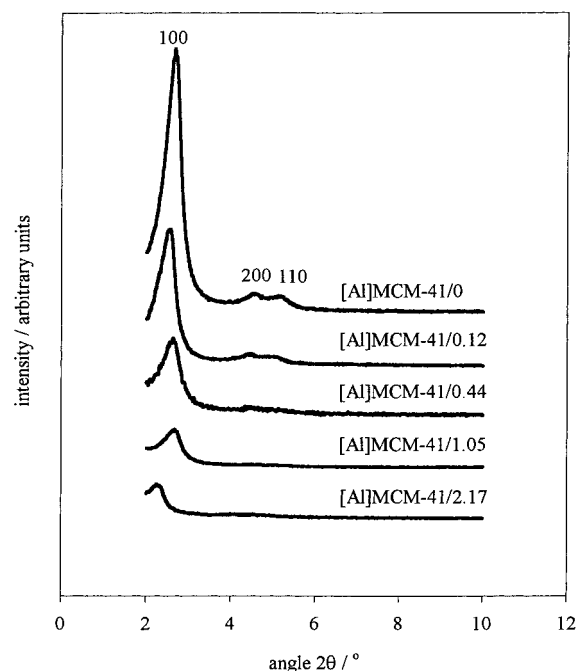

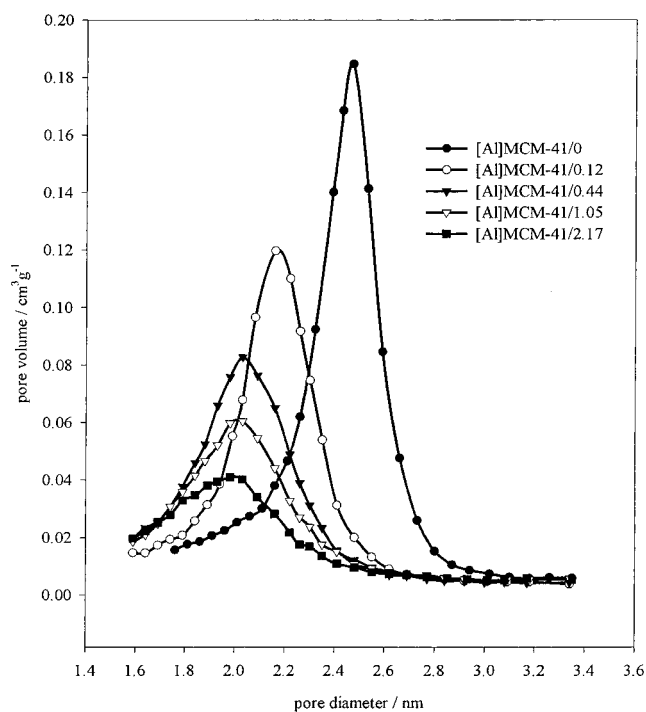**Figure 1.** XRD patterns of the parent [Al]MCM-41/0 material and of samples modified by ammonium fluoride.

Figure 2. Pore size distribution and pore volume of the parent [Al]-MCM-41/0 material and of samples modified by ammonium fluoride, derived from N_2 adsorption/desorption isotherms.

accompanied by a strong decrease of the pore volume from 0.19 to 0.04 cm^3/g (Figure 2). Considering the BET areas, however, up to a modification of the [Al]MCM-41 material with 0.44 mol NH_4F per gram, no decrease was observed. Hence, [Al]MCM-41 materials which were weakly modified with NH_4F keep their structure while for stronger treatments with NH_4F, a loss of the long-range order and a damage of the mesoporous structure occurs.

NMR Spectroscopic and Catalytic Investigations of Brønsted Acid Sites. To study the Brønsted acid sites of the parent and modified [Al]MCM-41 materials, ^1H MAS NMR spectros-
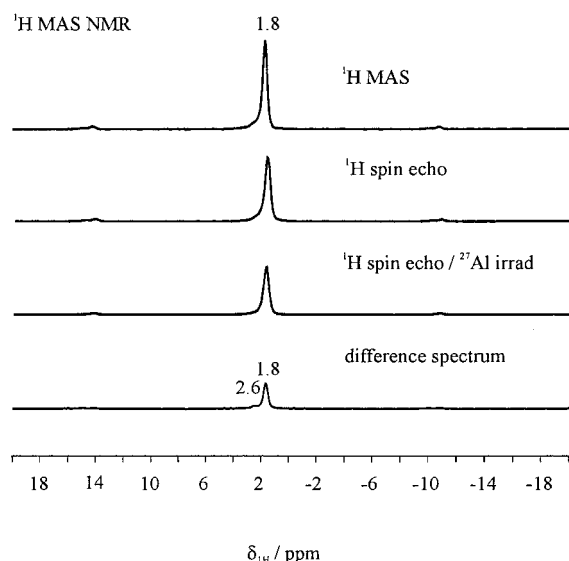
Figure 3. ^{1}H MAS NMR spectra of the dehydrated parent [Al]MCM-41/0 material, recorded by excitation with $\pi/2$ pulses (^{1}H MAS), Hahn-echo (^{1}H spin$-$echo), Hahn-echo and simultaneous irradiation of a ^{27}Al pulse (^{1}H spin$-$echo/^{27}Al irradiation), and the difference spectrum of the Hahn echo experiment without and with ^{27}Al irradiation (bottom).

copy of samples dehydrated at 673 K was performed. The ^{1}H MAS NMR spectra obtained (see, e.g., Figure 3, top) correspond to those reported in former investigations[4] and consist of a single signal at 1.8 ppm usually assigned to silanol groups at defect sites, e.g., in zeolites. The concentration of SiOH groups in mesoporous [Al]MCM-41 materials, however, is more than 1 order of magnitude larger than in zeolites.[4] The broad low-field flank of the signal of SiOH groups at 1.8 ppm is due to a small number of AlOH groups.

^{1}H{^{27}Al} TRAPDOR MAS NMR experiments are suitable to investigate the dipolar coupling between ^{1}H nuclei with spin $I = \frac{1}{2}$ and quadrupole nuclei such as ^{27}Al nuclei having a nuclear spin of $S = \frac{5}{2}$. If a ^{27}Al pulse is irradiated during the pulse delay of a Hahn echo sequence applied to ^{1}H nuclei, those ^{1}H nuclei contribute to the echo intensity only, which are not involved in a dipolar interaction with ^{27}Al nuclei. Subtraction of the ^{1}H spin$-$echo MAS NMR spectrum recorded with ^{27}Al irradiation (Figure 3, ^{1}H spin$-$echo/^{27}Al irrad) from the ^{1}H spin$-$echo MAS NMR spectrum obtained without ^{27}Al irradiation (Figure 3, ^{1}H spin$-$echo) gives a spectrum consisting of OH groups which are involved in a dipolar coupling with ^{27}Al nuclei. The difference spectrum shown in Figure 3, bottom, shows a weak signal at 2.6 ppm due to AlOH groups, but also a strong signal at 1.8 ppm caused by SiOH groups in the vicinity of aluminum atoms. These SiOH groups have a signal intensity, which corresponds to ca. 30% of the total SiOH intensity in the ^{1}H spin$-$echo MAS NMR spectrum (Figure 3, ^{1}H spin$-$echo).

A quantitative evaluation of the ^{1}H MAS NMR signal due to silanol groups in modified [Al]MCM-41 materials indicated a strong intensity decrease after the treatment with NH$_4$F. This is accompanied by a low-field shift of the resonance position from 1.8 ([Al]MCM-41/0) to 2.2 ppm ([Al]MCM-41/2.17). In Figure 4, the reduced number of SiOH groups, Δc_{OH}, is plotted as a function of the number of NH$_4$F, c_{NH4F}, introduced by the treatment. The corresponding curve shows an increasing fluoridation of SiOH groups up to a treatment with 0.44 mmol NH$_4$F per gram. After a stronger treatment with NH$_4$F, the decrease of the SiOH concentration becomes smaller. The latter observa-
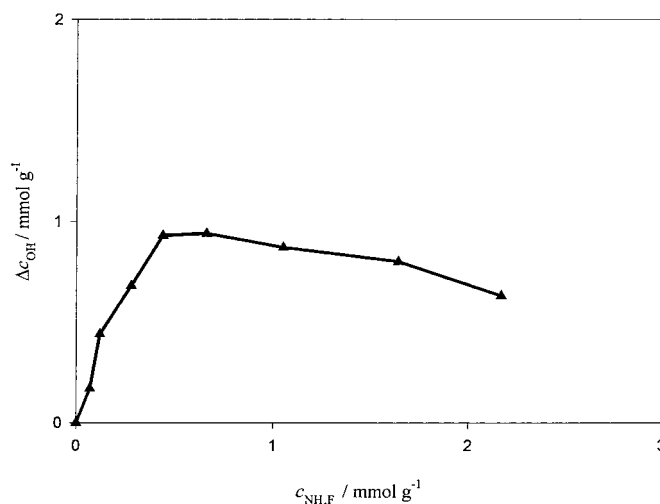

Figure 4. Number of fluoridated SiOH groups (Δc_{OH}), plotted as a function of the number of ammonium fluoride (c_{NH4F}) introduced by modification of the [Al]MCM-41 material.

tion may be due to a formation of additional defect SiOH groups caused by an increasing damage of the [Al]MCM-41 framework.

To quantify the number of Brønsted acid sites which have an acid strength suitable to protonate adsorbed bases, the adsorption of ammonia on modified and dehydrated [Al]MCM-41 materials was investigated by ^{1}H MAS NMR spectroscopy. Figure 5 shows the ^{1}H MAS NMR spectra of modified and dehydrated [Al]MCM-41 materials before (left) and after (right) adsorption of ammonia. The values given in Table 1, last column, were obtained by an evaluation of the intensity of the signal at ca. 6.7 ppm caused by the formation of ammonium ions on former Brønsted acid sites. The number of ammonium ions determined in this way increases up to a modification of the [Al]MCM-41 material with 0.44 mmol NH$_4$F per gram. After stronger treatments, the ammonium concentration decreases again and, finally, reaches the value of the parent [Al]MCM-41/0 material.

To clarify whether the fluoridation of [Al]MCM-41 materials is accompanied by an increase of the catalytic activity, the conversion of 2-propanol was investigated. At Brønsted and Lewis acid sites, dehydration of 2-propanol to propene and diisopropyl ether occurs while at base sites the dehydrogenation to acetone is the dominating reaction.[13] In the present work, the conversion of 2-propanol was performed on the most characteristic [Al]MCM-41 samples leading to propene as main reaction product and negligible amounts of diisopropyl ether only. In comparison with the parent [Al]MCM-41/0 material, a significant increase of the 2-propanol conversion, $X_{isopropanol}$, was obtained on the [Al]MCM-41 material treated with 0.44 mmol NH$_4$F per gram (Figure 6, left y-axis, filled triangles). On [Al]MCM-41 materials treated with more than 0.44 mmol NH$_4$F per gram, the conversion of 2-propanol decreased even below the value of the parent [Al]MCM-41/0 material. Interestingly, the qualitative behavior of the 2-propanol conversion, plotted as a function of the number of NH$_4$F introduced, c_{NH4F}, agrees well with the behavior of the number of ammonium ions, c_{NH4^+}, formed on Brønsted acid sites (Figure 6, right y-axis, open circles). Same relations were found for independently investigated series of [Al]MCM-41 materials treated with NH$_4$F.

Multinuclear Solid-state NMR Investigations of Framework Atoms in [Al]MCM-41 Materials. The ^{29}Si MAS NMR spectra of the parent and modified [Al]MCM-41 materials consist of three signals at ca. -91, -101, and -109 ppm (Figure
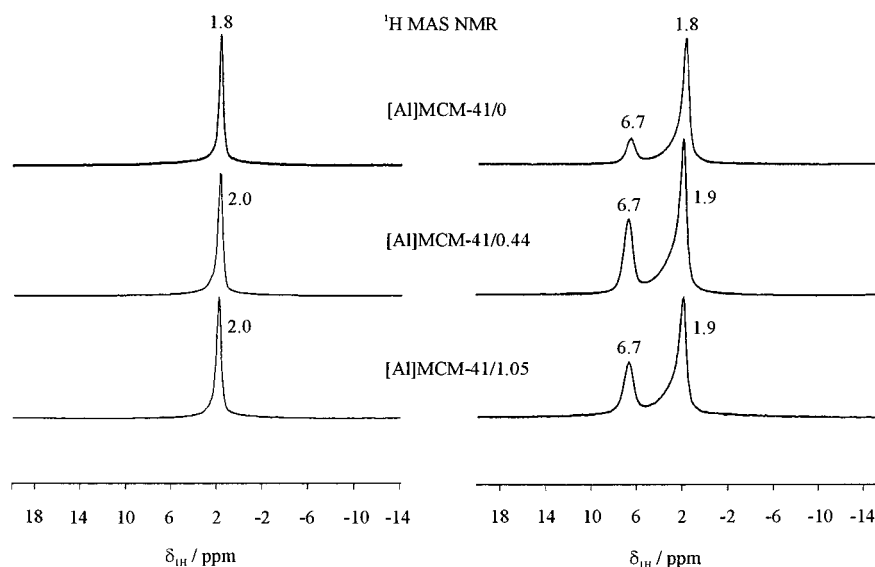
Figure 5. ^{1}H MAS NMR spectra of the parent [Al]MCM-41/0 material and of samples modified by ammonium fluoride, recorded after dehydration at 673 K, before (left) and after (right) adsorption of dry ammonia at room temperature and desorption at 473 K.
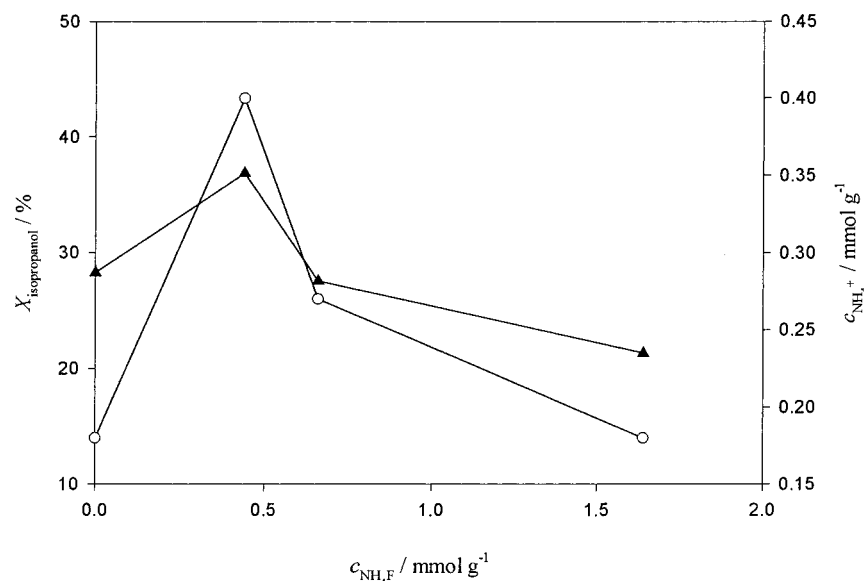

Figure 6. Number of ammonium ions formed by adsorption of ammonia on acid sites ($c_{NH_4^+}$, open circles) and conversion of 2-propanol ($X_{isopropanol}$, filled triangles), plotted as a function of the number of ammonium fluoride (c_{NH_4F}) introduced by a modification of the [Al]MCM-41 material.

7). According to Kolodziejski et al.,[14] the signal at -109 ppm is caused by Si(OSi)$_4$ and Si(OSi)$_3$OAl sites (Q^4), while the shoulders at -91 and -101 ppm are due to Si(OSi)$_2$(OH)$_2$ sites (Q^2) and Si(OSi)$_3$OH sites (Q^3) sites, respectively. As shown in Figure 7, a treatment of the [Al]MCM-41 material with NH$_4$F leads to a decrease of the Q^3 signal at -101 ppm. This decrease of the Q^3 signal, which is accompanied by an increase of the Q^4 signal at -109 ppm, corresponds to a transformation of Si-(OSi)$_3$OH sites to Si(OSi)$_4$ or Si(OSi)$_3$OAl sites.

To study the local structure of aluminum in [Al]MCM-41 materials, ^{27}Al spin−echo NMR and ^{27}Al MAS NMR spectroscopy were applied. MAS NMR spectroscopy yields spectra with a resolution, which is higher than that of spin−echo NMR spectra. However, spin−echo NMR spectroscopy is more suitable for the observation of broad signals such as those of aluminum atoms in a strongly disturbed oxygen coordination. The quadrupolar interaction of ^{27}Al nuclei (spin $S = \,^5\!/_2$) with the electric field gradient caused by a nonspherical charge distribution in the local structure leads to ^{27}Al NMR signals which renders an observation by NMR spectroscopy difficult.

In contrast to framework aluminum atoms in *hydrated* [Al]-MCM-41 materials, the framework aluminum atoms in *dehydrated* [Al]MCM-41 materials exist in a strongly asymmetric local structure. Therefore, their observation is hindered also by application of a spin−echo sequence (see Figure 7 in ref 4).

The ^{27}Al MAS NMR spectra of hydrated [Al]MCM-41 materials shown in Figure 8, left-hand side, consist of a signal at 53 ppm due to tetrahedrally coordinated aluminum species and a weak line at 0 ppm superposed by a broad signal at the same resonance position. The signals at 0 ppm are caused by octahedrally coordinated aluminum atoms. A treatment of the [Al]MCM-41 material with 0.44 mmol NH$_4$F per gram is accompanied by an increase of the intensity at 0 ppm. After a stronger treatment of the [Al]MCM-41 material with NH$_4$F, the signals at 0 ppm reach an intensity comparable with that of the signal at 53 ppm. The ^{27}Al spin−echo NMR spectra show a significantly stronger increase of the signal of octahedrally coordinated aluminum at 0 ppm after a treatment with 0.44 mmol NH$_4$F per gram. The differences between the MAS NMR and spin−echo NMR spectra indicate the presence of aluminum
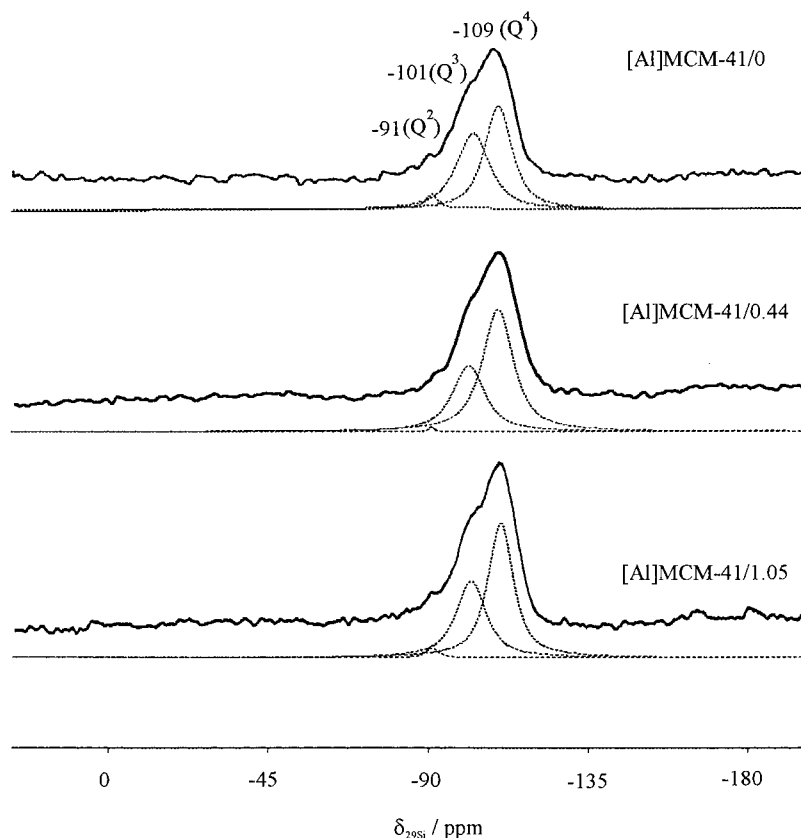
Figure 7. ^{29}Si MAS NMR spectra of the parent [Al]MCM-41/0 material and of samples modified by ammonium fluoride, recorded in the hydrated state.
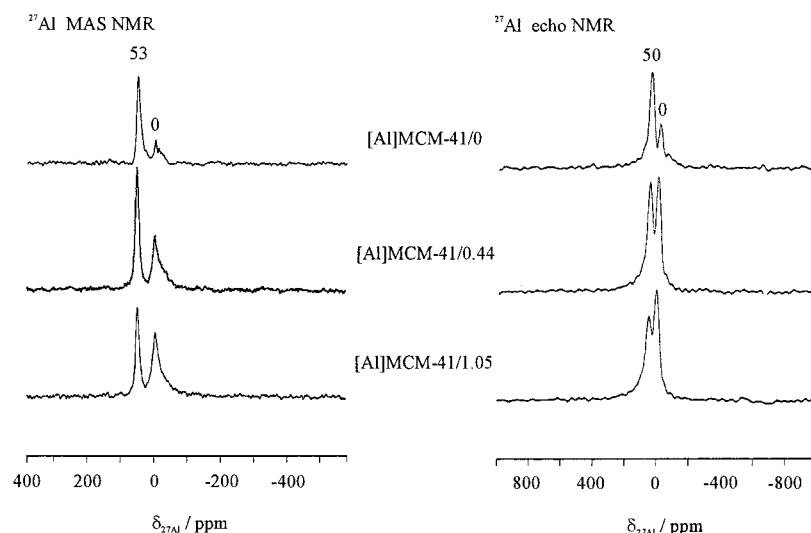

Figure 8. ^{27}Al MAS NMR (left-hand side) and ^{27}Al spin−echo NMR spectra (right-hand side) of the parent [Al]MCM-41/0 material and of samples modified by ammonium fluoride, recorded in the hydrated state.

atoms in a strongly disturbed octahedral coordination. This may be due to fluorine atoms bound to octahedrally coordinated aluminum atoms.

^{19}F MAS NMR spectroscopy allows a direct observation of the fate and behavior of fluorine atoms introduced into [Al]-MCM-41 materials. The ^{19}F MAS NMR spectra of hydrated [Al]MCM-41 materials shown in Figure 9 consist of up to three signals at −153, −155, and −156 ppm. The signal occurring at −156 ppm in the spectrum of [Al]MCM-41/0.44 is assigned to fluorine atoms in Si−F species.[15] Simultaneously, a signal appears at −155 ppm, which increases and dominates the ^{19}F MAS NMR spectra after a strong treatment with NH$_4$F.

According to the literature,[16] this signal is due to ^{VI}Al(O$_5$F) species. For the strongly modified [Al]MCM-41/1.64 material (Figure 9, bottom), a shoulder appears at −153 ppm which may be caused by additional aluminum−fluorine complexes formed in result of the partial damage of the [Al]MCM-41 material. Hence, ^{19}F MAS NMR spectroscopy of [Al]MCM-41/0.44 indicates an incorporation of fluorine atoms into at least two different local structures: One involves the formation of Si−F species and the other consists of ^{VI}Al(O$_5$F) species.

Local Structures of Aluminum and Fluorine Atoms in Modified [Al]MCM-41 Materials. ^{1}H MAS NMR and catalytic investigations performed in this work indicate that the treatment
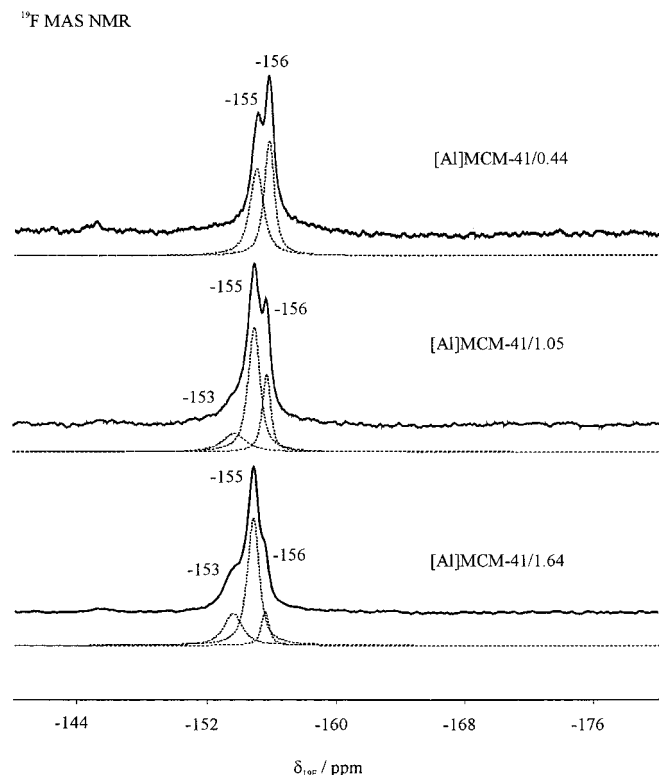
Acidity of Mesoporous [Al]MCM-41 Material

J. Phys. Chem. B, Vol. 106, No. 12, 2002 **3207**

Figure 9. ^{19}F MAS NMR spectra of the parent [Al]MCM-41/0 material and of samples modified by ammonium fluoride, recorded in the hydrated state.

of [Al]MCM-41 materials with NH$_4$F leads to the formation of OH groups with enhanced acid strength. However, these OH groups are not comparable with bridging OH groups (SiOHAl) in H-form zeolites causing ^{1}H NMR signals in the shift range of 3.8 to 4.3 ppm.[17] On the other hand, ^{27}Al NMR spectroscopy shows that the majority of aluminum atoms in the hydrated parent [Al]MCM-41/0 material exist in a tetrahedral oxygen coordination similar to that in microporous zeolites. Since in ammonium-exchanged [Al]MCM-41 material only a negligible number of sodium cations is present, the negative framework charges have to be compensated by ammonium ions and, after the deammoniation, by hydroxyl protons. However, in the ^{1}H MAS NMR spectra of deammoniated and dehydrated [Al]-MCM-41 materials, no signal of bridging OH groups occurs at 3.8 to 4.3 ppm. In contrast to tetrahedrally coordinated aluminum atoms in dehydrated zeolites which cause ^{27}Al quadrupolar patterns with characteristic singularities,[18] the ^{27}Al spin–echo NMR spectra of deammoniated and dehydrated [Al]MCM-41 materials consist of a very weak and broad ^{27}Al NMR signal only (see Figure 7 in ref 4). Hence, after the dehydration of [Al]MCM-41 materials, most of the framework aluminum should exist in a strongly disturbed tetrahedral or a 3-fold coordination. The asymmetric oxygen coordination of these aluminum atoms leads to a strong quadrupolar interaction and renders the observation of these aluminum atoms, also by ^{27}Al spin–echo NMR spectroscopy, difficult.

As indicated by the NMR spectroscopic data, the local structure of framework aluminum in the hydrated parent [Al]-MCM-41/0 material consists of tetrahedrally coordinated aluminum atoms (^{27}Al NMR signal at 53 ppm) which requires an OH bridge to a neighboring silicon atom (Scheme 1, local structure **I**). In the hydrated state, the hydroxyl proton of this OH bridge interacts with adsorbed water molecules. After dehydration (Scheme 1, local structure **II**), the OH bridge is transformed to a SiOH group contributing to the ^{1}H NMR signal

SCHEME 1
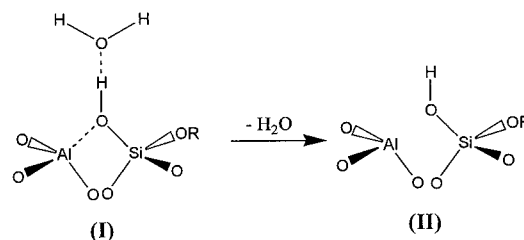
SCHEME 2
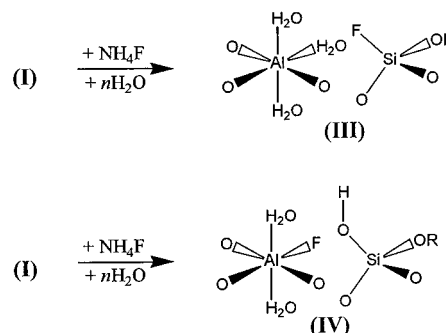
at 1.8 ppm. This model is supported by the ^{1}H{^{27}Al}TRAPDOR MAS NMR experiment (Figure 3), which indicated that ca. 30% of the SiOH groups in the parent [Al]MCM-41 material are located in the vicinity of aluminum atoms.

Treatment of [Al]MCM-41 materials with NH$_4$F, therefore, may attack the local structure **I** shown in Scheme 1. ^{19}F NMR spectroscopy of modified [Al]MCM-41 materials indicates that, after a weak treatment with NH$_4$F, Si−F species are formed. According to this model, the attack of NH$_4$F to the local structure **I** causes a fluoridation of the OH bridge (^{19}F NMR signal at −156 ppm). Hydration of the neighboring framework aluminum could lead to a tetrahedral or octahedral oxygen coordination (Scheme 2, local structure **III**). In the ^{1}H MAS NMR spectra of weakly modified and dehydrated [Al]MCM-41 materials, the fluoridation of the OH bridges leads to the decrease of the number of SiOH groups causing the ^{1}H NMR signal at ca. 1.8 ppm. After dehydration of the modified material, this process is accompanied by a recombination of vicinal SiOH groups as shown by the decrease of Q^3 sites in Figure 7. Simultaneously, a formation of ^{VI}Al(O$_5$F) species (Scheme 2, local structure **IV**) occurs. These species cause the ^{19}F NMR signal at −155 ppm and an increase of the ^{27}Al NMR signal at 0 ppm.

Assuming that R in Schemes 1 and 2 is a hydroxyl proton (Q^2 sites in Figure 7), the fluoridation of the OH bridge in the local structure **III** enhances the acid strength of the SiOH group remaining at the partially fluoridated silicon atom. After dehydration, the Si(O$_2$F)OH species formed in the vicinity of strongly disturbed framework aluminum are hydroxyl groups with enhanced acid strength. These are responsible for the low-field shift of the ^{1}H NMR signal of remaining silanol groups, the enhanced formation of ammonium ions after adsorption of ammonia and the improved catalytic activity in the conversion of 2-propanol.

After a strong treatment of [Al]MCM-41 with NH$_4$F, the local structure **IV** dominates. In this local structure, the fluorine atom is bound to the framework aluminum and does not directly influence hydroxyl protons existing at neighboring silicon atoms. Finally, a strong treatment of [Al]MCM-41 materials with NH$_4$F causes a damage of the local structure **I**, and the formation of additional defect SiOH groups occurs.

Conclusions

On bases of the NMR spectroscopic data obtained in this study, a local structure of aluminum species in the framework of hydrated [Al]MCM-41 materials is proposed which consists of tetrahedrally coordinated aluminum atoms (^{27}Al NMR signal at 53 ppm) involving an OH bridge to a neighboring framework silicon atom. After dehydration, these aluminum atoms have a strongly disturbed tetrahedral or a 3-fold oxygen coordination. The treatment of this [Al]MCM-41 material with ammonium fluoride cause a fluoridation of the OH bridge which leads to the formation of Si−F species (^{19}F NMR signal at −156 ppm). Simultaneously, a fluoridation of framework aluminum and a formation of ^{VI}Al(O$_5$F) species occurs (^{19}F NMR signals at −155 ppm, ^{27}Al NMR signal at 0 ppm). Hydroxyl groups bound to partially fluoridated silicon atoms (Si−F species) are characterized by an enhanced acid strength. These Si(O$_2$F)OH species act as Brønsted acid sites and are responsible for a low-field shift of the ^{1}H NMR signal of remaining silanol groups, an enhanced formation of ammonium ions after adsorption of ammonia and an improved catalytic activity in the conversion of 2-propanol. A strong treatment of [Al]MCM-41 materials with NH$_4$F, on the other hand, causes a damage of the mesoporous structure and a loss of the catalytic activity of this material.

References and Notes

(1) Kresge, C. T.; Leonovicz, M. E.; Roth, W. J.; Vartulli, J. C.; Beck, J. S. *Nature* **1992**, *359*, 710.

(2) Biz, S.; Occelli, M. L *Catal. Rev. −Sci. Eng.* **1998**, *40*, 329.

(3) Ghanbari-Siahkali, A.; Philippou, A.; Dwyer, J.; Anderson, M. W. *Appl. Catal. A* **2000**, *192*, 27.

(4) Hunger, M.; Schenk, U.; Breuninger, M.; Glaeser, R. Weitkamp, J. *Microporous Mesoporous Mater.* **1999**, *27*, 261.

(5) Corma, A.; Grande, M. S.; Gonzalez-Alfaro, V.; Orchills, A. V. *J. Catal.* **1996**, *159*, 375.

(6) (a) Mokaya, R.; Jones, W.; Luan, Z.; Alba, M. D.; Klinowski, J. *Catal. Lett.* **1997**, *45*, 259. (b) Koch, H.; Liepold, A.; Roos, K.; Stoecker, M.; Reschetilowski, W. *Chem. Eng. Technol.* **1999**, *22*, 10.

(7) Kosslick, H.; Lischke, G.; Walther, G.; Storek, W.; Martin, A.; Fricke, R. *Microporous Mater.* **1997**, *9*, 13.

(8) Borade, R. B.; Clearfield, A. *J. Chem. Soc., Faraday Trans.* **1995**, *91*, 539.

(9) Ghosh, A. K.; Kydd, R. A. *Zeolites* **1990**, *10*, 766.

(10) Glaeser, R. Ph. D. Thesis, Faculty of Chemistry, University of Stuttgart, 1997.

(11) Freude, D. *Chem. Phys. Lett.* **1995**, *235*, 69.

(12) Wolf, I.; Freude, D. *Microporous Mater.* **1995**, *5*, 69.

(13) Gervasini, A.; Auroux, A. *J. Catal.* **1991**, *131*, 190.

(14) Kolodziejski, W.; Corma, A.; Navarro, M.-T.; Perez-Pariente, J. *Solid State Nucl. Magn. Reson.* **1993**, *2*, 253.

(15) Delmotte, L.; Soulard, M.; Guth, F.; Seive, A.; Lopez, A.; Guth, J. L. *Zeolites* **1990**, *10*, 778.

(16) Fischer, L.; Harlé, V.; Kasztelan, S.; d'Espinose de la Caillerie, J.-B. *Solid State Nucl. Magn. Reson.* **2000**, *16*, 85.

(17) Hunger, M. *Catal.−Rev. Sci. Eng.* **1997**, *39*, 345.

(18) Freude, D.; Ernst, H.; Wolf, I *Solid State Nucl. Magn. Reson.* **1994**, *3*, 271.